frontiers | Frontiers in Chemistry

TYPE Original Research
PUBLISHED 09 November 2023
DOI 10.3389/fchem.2023.1287883

OPEN ACCESS

EDITED BY
Behrooz Maleki,
University of Mazandaran, Iran

REVIEWED BY
Milad Ghani,
University of Mazandaran, Iran
Shanker Govindaswamy,
Bangalore University, India

*CORRESPONDENCE
Hoda A. Ahmed,
ahoda@sci.cu.edu.eg

RECEIVED 02 September 2023
ACCEPTED 30 October 2023
PUBLISHED 09 November 2023

CITATION
Ahmed HA, Abolibda TZ, Ismail YAM, Almohammedi A, Aly KA, Ibrahim MS and Gomha SM (2023), Novel maleic anhydride derivatives: liquid crystalline materials with enhanced mesomorphic and optical characteristics.
Front. Chem. 11:1287883.
doi: 10.3389/fchem.2023.1287883

Novel maleic anhydride derivatives: liquid crystalline materials with enhanced mesomorphic and optical characteristics

Hoda A. Ahmed[1,2]*, Tariq Z. Abolibda[3], Yasser A. M. Ismail[4], Abdullah Almohammedi[4], K. A. Aly[5,6], Mohamed S. Ibrahim[3] and Sobhi M. Gomha[3]

[1]Department of Chemistry, Faculty of Science, Cairo University, Giza, Egypt, [2]Chemistry Department, College of Sciences, Taibah University, Yanbu, Saudi Arabia, [3]Department of Chemistry, Faculty of Science, Islamic University of Madinah, Madinah, Saudi Arabia, [4]Department of Physics, Faculty of Science, Islamic University of Madinah, Madinah, Saudi Arabia, [5]Department of Physics, Collage of Science and Arts Khylais, University of Jeddah, Khulais, Saudi Arabia, [6]Department of Physics, Faculty of Science, Al-Azhar University, Assiut Branch, Assiut, Egypt

A new class of liquid crystalline materials, 4-(2,5-dioxo-2,5-dihydro-1*H*-pyrrol-1-yl)phenyl 4-(alkoxy)benzoates (Mn), derived from maleic anhydride, was synthesized and studied for mesomorphic and optical properties. These materials consist of three derivatives with varying terminal flexible chain lengths (6–12 carbons) linked to the phenyl ring near the ester bond. The study employed differential scanning calorimetry and polarized optical microscopy (POM) to characterize the mesomorphic properties. Molecular structures were elucidated using elemental analysis, FT-IR, and NMR spectroscopy. The findings reveal that all the synthesized maleic anhydride derivatives exhibit enantiotropic nematic (N) mesophases. The insertion of the heterocyclic maleic anhydride moiety into the molecular structure influences the stability and range of the N phase. Additionally, entropy changes during N-isotropic transitions are of small magnitude and exhibit non-linear trends independent of the terminal alkoxy chain length (n). This suggests that the ester linkage group does not significantly promote molecular biaxiality, and the clearing temperature values are relatively high. By comparing the investigated materials with their furan derivatives found in existing literature, it was established that the substitution examined in this study induces the formation of nematic phases.

KEYWORDS

liquid crystal, maleic anhydride, N-arylmaleimide derivatives, nematic phase, transition entropy

1 Introduction

Today, all types of display devices, including computer and laptop displays, TVs, clocks, visors, and navigational systems, use liquid crystals. When a substance is in a liquid crystal state, it possesses characteristics of both liquids and crystals. Their novel optical, electrical, and mechanical features have garnered a lot of interest. Each liquid crystal assembly that

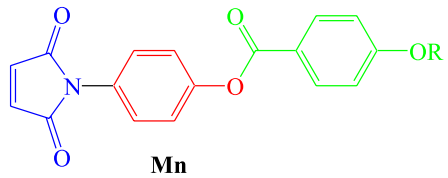

Mn

(**M6,** R = C_6H_{13}; **M8,** R = C_8H_{17}; **M10,** R = $C_{10}H_{21}$; **M12,** R = $C_{12}H_{25}$)

GRAPHICAL ABSTRACT

makes up a display pixel is governed by its own electromagnetic field. The field modifies the liquid crystals' orientation, which alters how much light can pass through them and result in the images you see on a screen (Alamro et al., 2021; Gomha et al., 2021; Abdou et al., 2022; Alamro et al., 2022; Chi et al., 2022; Uchida et al., 2022; Wang et al., 2022; Yin et al., 2022; Behera et al., 2023; Ma et al., 2023).

The greater coast and lower conversion efficiency of solar energy now restrict its application. One of the most crucial areas to investigate for cutting costs and boosting conversion efficiencies in solar systems is the performance of several basic organic derivatives (Zhang et al., 2018; Li et al., 2019). Solar energy applications such catalytic photodegradation of dyes, solar hydrogen generation, photo-electrochemical water splitting, and solar cells rely heavily on band gap engineering and optical property management (Ahmed et al., 2020).

In recent times, maleimides have gained recognition as significant pharmacophores and have assumed a crucial role as medicinal agents, exhibiting diverse biological activities. These activities encompass antibacterial properties (López et al., 2003), analgesic effects (Mahle et al., 2010), antistress attributes (Badru et al., 2012), antiprotozoal capabilities (Dürüst et al., 2012), antiangiogenic functions (Acero et al., 2012), as well as cytotoxicity, DNA binding, and apoptotic inducing activity (Alaa, 2007a). Various derivatives of maleimides have been identified as selective inhibitors of specific enzymes, including monoglyceride lipase (Matuszak et al., 2009), GSK-3a (Sivaprakasam et al., 2006), Cdc25B (Chen et al., 2010), Bfl-1 (JCashman et al., 2010), and DNMT-1 (Suzuki et al., 2010). The synthesis and biological evaluation of N-aryl maleimide analogs have been extensively explored. N-aryl maleimides serve as the structural framework for numerous natural products such as polycitrin (Burtoloso et al., 2006) and camphorataimides (Stewart et al., 2007). Maleimide and its derivatives are synthesized from maleic anhydride through a process involving treatment with amines followed by dehydration (Birkinshaw et al., 1963). Maleimide derivatives exhibit significant appeal in terms of their chemical reactivity. They participate in fascinating reactions like Diels–Alder reactions with dienes and nucleophilic Michael-type additions of thiols or amines to the vinylene moiety. The unsaturated imide serves as a crucial building block in organic synthesis. Moreover, maleimide encompasses a group of derivatives derived from the potent maleimide, wherein the NH group is substituted with alkyl or aryl groups such as methyl or phenyl, respectively. Additionally, the vinylene group within the maleimide moiety, featuring a 1,2-disubstituted ethylene structure, can undergo polymerization with radical or anionic initiators. This process yields a polymer with exceptional thermostability or heat-resisting properties, which can be further copolymerized with vinyl acetate (A et al., 2014).

The addition of a fused-heterocycle moiety to the molecular structure has been thoroughly examined in the quest to create new mesogenic cores, and the results show a variety of novel mesomorphic features (Han, 2013; Ghosh and Lehmann, 2017). In addition to increasing the species of liquid crystals, the addition of heteroatoms like nitrogen, sulphur, and oxygen also has a significant impact on the thermal and geometrical properties of the materials under investigation (Seed, 2007; Ha et al., 2010; Tariq et al., 2013; Merlo et al., 2018; Yeap et al., 2018; Weng et al., 2019a; Weng et al., 2019b; Ren et al., 2019). Insertion of fused-aromatic rings into a central or terminal structural shape alters the dielectric constant, polarizability, geometry, and mesophase transition temperatures (Seed, 2007; Ha et al., 2010; Tariq et al., 2013; Merlo et al., 2018; Yeap et al., 2018; Weng et al., 2019a; Weng et al., 2019b; Ren et al., 2019; Nafee et al., 2020a). Compounds contain imide groups, whether small molecules or macromolecules, display impressive electrical properties, favorable solubility in polar substances, resistance to hydrolysis, and high thermal stability (Bharel et al., 1993; Iijima et al., 1995; Langmuir et al., 1995; Hamper et al., 1996; Ohkubo et al., 1996; Bojarski et al., 2004; Alaa, 2007b; Mohammed and Mustapha, 2010a). These exceptional characteristics have prompted significant efforts to develop various imide-containing compounds composed of two carbonyl groups bonded to a nitrogen atom. The conventional method for synthesizing cyclic imides without substitutions involves heating dicarboxylic acids or their anhydrides with reactants such as ammonia, urea, formamide, lithium nitride, or primary amines (Handley et al., 1960; Gordon and Ehrenkaufer, 1971; Połoński et al., 2000; Wu et al., 2003). However, this reaction necessitates high temperatures to ensure efficient ring closure.

New classes of materials, liquid crystalline thermosets (LCTs) bring together the best qualities of thermotropic LC polymers and traditional thermosets. The network structures of these materials are made up of rigid-rod or extended chain segments that are cross-linked in three dimensions. Increased processability, higher glass transition temperatures, greater dielectric strength, and less shrinkage during curing are only a few of the benefits of LCTs (Lee et al., 2002; Jang and Bae, 2005; Cho et al., 2006). Additionally, they exhibit noteworthy qualities such as extremely low dielectric constants and dissipation factors, exceptional performance at high temperatures, chemical resistance, inherent flame retardance (Lee, 2006; Wang and Jiang, 2006), and low coefficients of thermal expansion (CTEs). These unique properties make LCTs highly desirable for advanced electronic applications. Moreover, efforts have been made to reduce the CTEs of LCT films in order to mitigate thermal stress in electronic laminates used in microelectronic applications (Hasegawa and Tominaga, 2005; Hasegawa et al., 2006; Morita et al., 2006). Functionalized rigid-rod oligomers or

monomers are cross-linked in the mesophase to form either an isotropic or anisotropic network structure; these materials are known as thermotropic liquid crystals (LCs). Some thermotropic LCTs have been reported to possess cross-linkable units as end groups. Various functional units have been utilized as such end groups, including maleimide (Hoyt et al., 1990a), nadimide (Hoyt et al., 1990b), epoxy (Domszy and Shannon, 1990; Mallon and Adams, 1993; Carfagna et al., 1994a; Carfagna et al., 1994b; Carfagna et al., 1997), isocyanate (Mormann and Zimmermann, 1995), and acetylene (Langlois et al., 1994; Benicewicz et al., 1997; Gavri et al., 2001). Due to the importance of intermolecular interactions between mesogens in formation the liquid crystal phase, this characteristic is essential for the production of ordered structures in liquid crystals. Additionally, the aromatic rings also engage in - stacking interactions, which further improve the mesogen's ordering capacity.

The purpose of this research, which is a continuation of our earlier work, is to create new derivatives of the terminal heterocyclic moiety, specifically 4-(2,5-dioxo-2,5-dihydro-1*H*-pyrrol-1-yl) phenyl 4-(alkoxy)benzoates, **Mn**. An ester linkage with a phenyl ring connected to various lengths of alkoxy groups and the other terminal is the maleic anhydride moiety. The project also aims to examine the mesomorphic and optical characteristics of the current system and investigate the impact of changing the flexible chain's terminal length on their mesomorphic interaction.

2 Results and discussion

2.1 Synthesis

The process used to create the titled **Mn** compounds involves two sequential steps. It begins with synthesizing 1-(4-hydroxyphenyl)-1*H*-pyrrole-2,5-dione **3** by combining 4-hydroxyaniline **2** with maleic anhydride **1** as previously reported (Mohammed and Mustapha, 2010a). Next, compound **3** is transformed into the desired 4-(2,5-dioxo-2,5-dihydro-1*H*-pyrrol-1-yl)phenyl 4-(alkoxy)benzoates by reacting it with 4-alkoxybenzoic acid **4** in dry methylene chloride, along with N,N′-dicyclohexylcarbodiimide (DCC) and catalytic amounts of 4-dimethylaminopyridine (DMAP) (Scheme 1). The structure of compounds **Mn** was confirmed using elemental analyses and spectral data, including IR, ^{1}H NMR, ^{13}C NMR and MS.

2.2 Spectroscopic analysis

The ^{1}H-NMR data provided essential structural information about the synthesized compounds **Mn**, confirming the successful synthesis of the intended product and the presence of characteristic functional groups. The ^{1}H-NMR spectrum (300 MHz, $CDCl_3$) of compound **M6** exhibited distinct peaks at δ/ppm values. The signals at 0.73–0.80 ppm were attributed to a triplet (t) representing the presence of three equivalent methyl protons (CH_3). Additionally, a multiplet (m) pattern between 1.22 and 1.43 ppm indicated six protons arising from the aliphatic chain ($CH_3(CH_2)_3CH_2CH_2O$-). Two more protons of this chain resonated as a multiplet in the range of 1.70–1.76 ppm. A triplet at 3.79–4.04 ppm corresponded to two protons associated with the methylene group of the aliphatic chain ($CH_3(CH_2)_3CH_2CH_2O$-). In the aromatic region, three distinct doublets (d) were observed at 7.15, 7.24, and 7.37 ppm, each representing two protons of the aromatic ring. Additionally, a sharp singlet (s) appeared at 7.74 ppm, indicating the presence of two protons from the pyrrole moiety. Finally, another doublet at 8.12 ppm accounted for two protons of the aromatic ring.

Moreover, the ^{13}C-NMR data provided valuable insights into the structural features of the unknown compounds, confirming the successful synthesis of the desired molecule and supporting its potential application in various biological and chemical studies. The ^{13}C-NMR spectrum (75 MHz, $CDCl_3$) of compound **M6** exhibited distinct peaks at various chemical shifts. The signal at 14.0 ppm were assigned to the methyl (CH_3) group, while the peaks at 23.8, 25.6, 29.57, 31.0, and 68.2 ppm corresponded to the methylene (CH_2) groups in the molecule. The resonances observed at 116.2, 121.5, 123.0, 127.9, 130.2, 131.5, 136.0, and 147.5 ppm were attributed to the aromatic carbon atoms (Ar-C) and the carbon-nitrogen (C=N) groups present in the structure. Additionally, signals at 161.6 ppm indicated the presence of conjugated double bonds involving aromatic carbons and C=N. Moreover, the signals at 163.1 and 166.3 ppm were attributed to the two carbonyl (C=O) carbon atoms.

Additionally, the infrared spectrum (IR) spectral data provide valuable insights into the molecular structure and functional groups present in the compound, aiding in its characterization and potential application in various fields. The infrared spectrum of compound **M6** recorded in KBr disc displayed characteristic vibrational bands at v3041 cm^{-1}, corresponding to (=C-H) stretching vibrations, and at 2928 cm^{-1}, attributed to (-C-H) stretching vibrations. Additionally, two prominent peaks were observed at 1686 cm^{-1} and 1729 cm^{-1}, indicating the presence of two carbonyl groups (2 C=O) within the molecule. Furthermore, a peak at 1605 cm^{-1} was observed, which can be attributed to the stretching vibration of the carbon-nitrogen double bond (C=N), while a band at 1571 cm^{-1} signifies the presence of carbon-carbon double bonds (C=C).

Finally, the MS data provides valuable insights into the fragmentation pattern and molecular structure of compound **Mn**, aiding in its characterization and identification for further studies and potential applications. The results of the mass spectrometry (MS) analysis of compound **M6** revealed a molecular ion peak at m/z 393, corresponding to the intact molecular weight of the compound (M^+). Another significant peak at m/z 307 was observed with 100% relative intensity, likely resulting from the loss of the hexyl group (C_6H_{13}) from the parent molecule. Moreover, the peak at m/z 292 (71%) suggests the further fragmentation of the compound. Other notable peaks included m/z 231 (63%) indicating possible fragmentation involving the phenyl pyrrole moiety, m/z 189 (38%) suggesting the loss of both the hexyl and phenyl pyrrole moieties, and m/z 162 (81%) representing a common fragment found in the MS analysis.

2.3 Mesomorphic examinations

DSC and POM measurements have been used to examine the phase transitions and optical properties of the synthesized **Mn** derivatives under investigation. Figure 1 shows an example of a representative DSC thermogram for the proposed compound **M12** after heating and

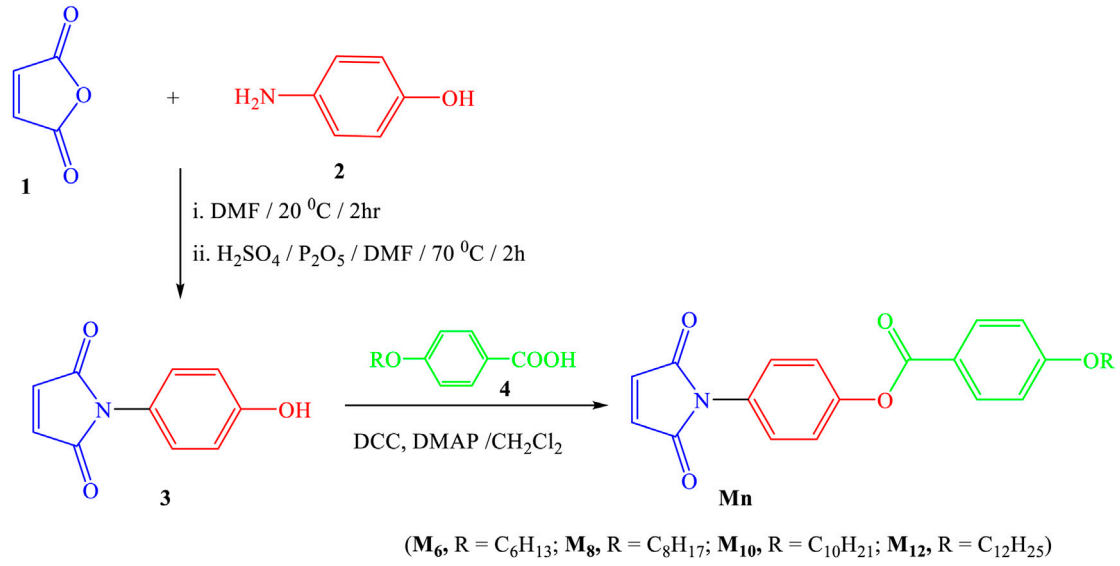

SCHEME 1
Synthesis route of title compounds **Mn**.

cooling cycles. It is clearly shown that upon heating, the compound **M12** showed two endotherms characteristic of the crystal–N and N–isotropic transitions. While, during the cooling cycle, the compound exhibits nematic phase but its freezing transition temperature is shifted to lower temperature. DSC measurements show two transition peaks that change depending on the **Mn** structural form of the produced materials. Additionally, for all chain lengths (n), the mesomorphic transfers from Cr to N upon heating and N to I upon cooling. According to the attached terminal flexible chain length moiety, which is associated with the mesomorphic interaction, significant endothermic and exothermic peaks were seen, and the cooling cycle corroborated those peaks when the temperature was lowered. The results of the DSC were verified by optical textures under POM. The POM measurements revealed textures which confirmed N mesophases. Figure 2 showed how the **M12** images were derived. Table 1 provides an overview of the mesomorphic transition temperatures and corresponding enthalpies for all the synthesized maleic anhydride derivatives, **Mn**, as determined by DSC analysis. Figure 3 shows their relationships in order to explore how the length of the terminal alkoxy chain (n) affects the mesomorphic behavior of produced compounds. Table 1 and Figure 3 showed that the mesomorphism of all synthesized members of the maleic anhydride derivatives **Mn**, as well as their high mesomorphic thermal stability and good mesophase range, are reliant on the length of their terminal flexible chains. Additionally, all investigated molecules of **Mn** series have a pure N phase and are enantiotropic. Additionally, Table 1 and Figure 3 show that the melting point of compounds varies arbitrarily with chain length (n). The member with the shortest terminal length (**M6**) has the highest nematic thermal stability and enantiotropic N phase at temperatures of 153.9 and 46.4°C, respectively. While the range and nematic stability of the compound **M8** are around 144.6 and 27.4°C, respectively. Enantiotropic N mesophase with nematogenic stability and a range of nearly 132.9 and 20.2°C is also present in the **M10** derivative. Finally, compared to **M8** and **M10**, the derivative with the greatest chain length (**M12**) has a higher mesomorphic range (33.5 C) and weaker thermal N stability (126.8°C). In general, the electronic properties of the terminal substituents have a significant influence on the molecular architecture, polarizability, and dipole moment of the proposed materials. Additionally, an increase in the polarity and/or polarizability of the molecular mesogenic cores has an impact on the mesomorphic nature. The examined homologue's mesomorphic range expanded in the following order: **M6** > **M12** > **M8** > **M10**. How molecular-molecular interactions affect the mesomorphic behavior of rod-like molecules depends on the geometrical form of the polar terminal groups and the heterocyclic moieties in the molecule (Nafee et al., 2020b). The present prepared group exhibited purely N mesophases, and the N phase stability decreased with n. The interaction between the mesogenic units was reduced as the chain length increased, lowering the N-I transition temperature. The observations of mesomorphic qualities are the result of the sharing of these factors to various degrees. The kind of the observed mesophase is mostly determined by the end-to-end aggregation caused by the oxygen of the alkoxy chain, the ester carbonyl moiety, and the side-by-side cohesive interactions between molecules (Gray, 1962; Luckhurst and Gray, 1979). In general, mesophase stability is enhanced by increasing the polarizability and/or polarity of the entire mesogenic component of the molecule. Although the rod-shaped molecule is less rigid, the increased anisotropic features improve mesophase stability (Yelamagg et al., 2007; Pradhan et al., 2017; Nayak et al., 2019; Sunil et al., 2020). An increase in the alkoxy terminal chain is also projected to reduce stability by diluting the mesogenic core.

2.4 Entropy changes

Entropy is a crucial factor that must be taken into account while engineering phase transition temperatures. As a result, it is essential to concentrate more on thermodynamic factors in order to create alternative plans for lowering melting and clearing temperatures to

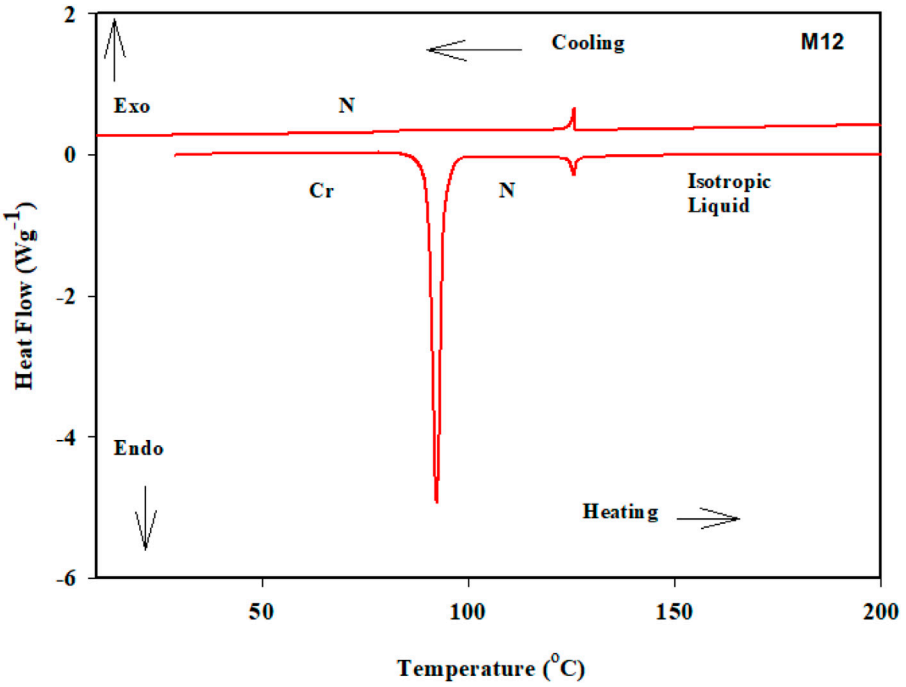

FIGURE 1
DSC thermograms of **M12** recorded from the second heating and cooling scans at rate ± 10°C/min.

FIGURE 2
Textures observed under POM for compound **M12** of (a) N phase at 120.0°C upon heating and.

TABLE 1 Phase transition temperatures, °C (enthalpy of transition ΔH, kJ/mole), mesomorphic range (ΔT, °C) and the normalized entropy of transition, ΔS/R, for present series Fn.

Comp	$T_{Cr\text{-}N}$	$\Delta H_{Cr\text{-}N}$	$T_{N\text{-}I}$	$\Delta H_{N\text{-}I}$	ΔT_N	$\Delta S_{N\text{-}I}/R$
M6	107.5	51.60	153.9	2.76	46.40	0.78
M8	117.2	47.82	144.6	2.64	27.40	0.76
M10	112.7	41.93	132.9	2.10	20.20	0.62
M12	93.3	44.10	126.8	2.15	33.50	0.65

Cr-N, solid—nematic transition.
N-I = nematic—isotropic liquid transition.
R is the universal gas constant.

levels that complex mesogens can tolerate. Since G = 0, phase transitions are often order-disorder transitions for which H = TS. As a result, the transition entropies can be obtained from the estimated transition enthalpies obtained using differential scanning calorimetry. These are undoubtedly produced as a result of interaction energy attenuation.

Sorai and Saito observed, The alkyl chain can acquire a substantial amount of entropy during disordering, which changes the relative thermodynamic stability of aggregated states (Sorai and Saito, 2003). These chains are incredibly mobile in liquid crystals and act as a sort of solvent. They also explained how the type of phase affects how ordered aliphatic chains are. For instance, the chains have a tendency to be more ordered in lamellar phases compared to cubic bicontinuous phases, whereas the mesogen cores are more disordered in lamellar phases and ordered in cubic phases. Entropy from the chain reservoir can therefore be transported to the core in the scenario where cubic bicontinuous phases change into a lamellar phase. In general, phase transition temperatures can be engineered using the substantial entropy change that results from increasingly ordered chains sequentially increasing entropy until they reach their full degree of freedom in the isotropic phase. Low melting temperatures were ensured by the significant entropy changes at the crystal-liquid crystal transitions of various kinds of mesogens.

Table1 lists the normalized transition entropy changes, or $\Delta S_{N\text{-}I}/R$, of the currently studied homologues (**Mn**). The results

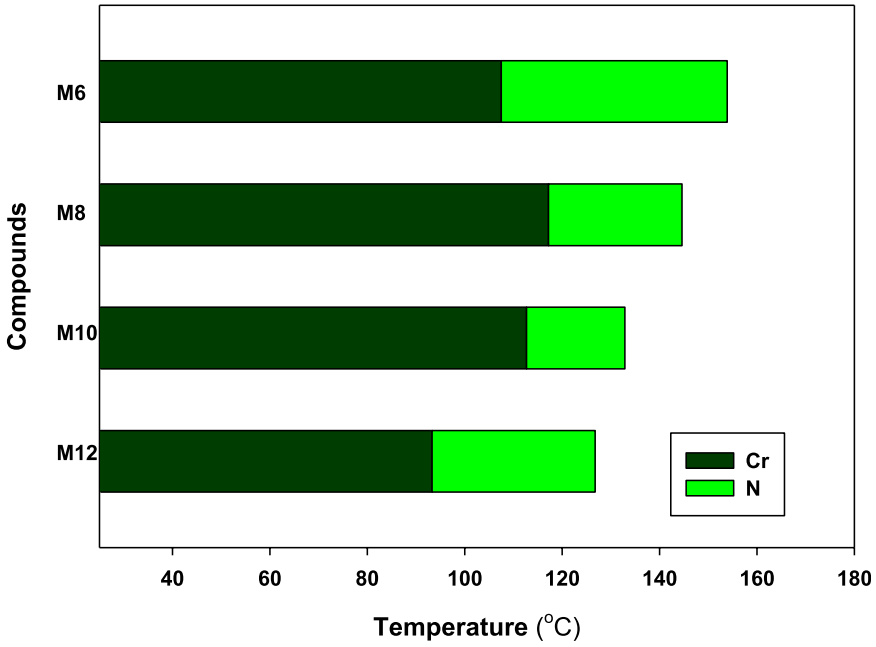

FIGURE 3
Effect of terminal side alkoxy chain length (n) on mesomorphic characteristics of the **Mn** derivatives of maleic anhydride studied.

demonstrated that extremely modest entropy variations were found, which were primarily dependent on the type of terminal substituents and msogenic cores. Because of their decreased anisotropy as a result of their molecular geometry and molecular biaxiality, the observed modest values can be explained (Yeap et al., 2011; Henderson et al., 2005; Yeap et al., 2015; Attard et al.). The creation of the mesophase and the molecular organization depend on the molecular orientation, which is influenced by the induction, conjugation forces, particular dipolar contacts, and - stacking interactions (Yeap et al., 2011; Henderson et al., 2005; Yeap et al., 2015; Attard et al.). An increase in dipolar ordering and a decrease in dipolar entropy arise from applying an electrical field to a polar insulator. The dielectric material will return to a less ordered dipolar state once the field is withdrawn, increasing the dipolar entropy (Shanker and Yelamaggad, 2011). In addition, it is more likely to realize a high the electrocaloric effect if the dipolar materials are operated near dipolar order-disorder transitions, where a dipolar ordered state can be created from a dipolar disordered state.

2.5 Comparative analysis with related derivatives

It is important to compare the examined materials to analogous ones that have been previously reported with another moiety having the furan substitution as terminal moiety (**Fn**) (Alshabanah et al., 2021) in order to understand the effect of the terminal maleic anhydride moiety on the phase behavior of the materials. Across all parallel series, the maximum allowed number of carbon atoms in the terminal chain (n) was 6, 8, or 12. According to recent findings (Alshabanah et al., 2021), the **Fn** series are intrinsically mesomorphic, exhibiting high mesomorphic thermal stability and a decent mesophase range that varies with the terminal flexible chain length. While molecules **F6** and **F10** are enantiotropic and have pure N phases, the longer chain derivative **F12** contains two mesomorphic transitions (SmA and N phases). The dimorphic characteristics of **F12** demonstrate the existence of an enantiotropic N mesophase and a monotropic SmA phase. However, the nematic phases of the maleic anhydride compounds **Mn** cover all side chain lengths. It is evident that the kind of LC phase has a substantial influence on the terminal replacement. Because only N phases were seen in the maleic anhydride derivatives, the mesomorphic properties were changed when the terminal side by the furan moiety, and the SmA phase developed for lengthy terminal side chain members.

3 Experimental

3.1 Synthesis

The process used to create the titled Mn compounds involves two sequential steps (Scheme 1):

3.1.1 Synthesis of 1-(4-hydroxyphenyl)-1*H*-pyrrole-2,5-dione, 3

P-Aminophenol (1.637 g, 0.015 mol) and maleic anhydride (1.471 g, 0.015 mol) were separately dissolved in 5 mL of DMF, resulting in solutions A and B, respectively. Solution B was slowly added to solution A, forming solution C. Solution C was then stirred at 20°C in a water bath for 2 h. Next, P_2O_5 (1.2 g) was dissolved in a mixture of 1 mL of H_2SO_4 and 7 mL of DMF. This mixture was gradually added to solution C while stirring, and the entire solution was further stirred for 2 h at 70°C. To cool the mixture, it was placed

in an ice bath and then poured into cold water. Upon precipitation, a solid formed, which was subsequently filtered, washed with distilled water, and finally recrystallized from 2-propanol. The resulting crystals were dried in a vacuum oven at 65°C for 24 h. Yield: 84%; m. p. 184°C–186°C (Lit. m. p. 182°C–184°C (Mohammed and Mustapha, 2010b)).

3.1.2 General procedure for synthesis of 4-(2,5-dioxo-2,5-dihydro-1*H*-pyrrol-1-yl)phenyl 4-(alkoxy)benzoates, Mn

A mixture consisting of 1-(4-hydroxyphenyl)-1H-pyrrole-2,5-dione **3** (1.89 g, 10 mmol) and the appropriate derivatives of 4-alkoxy benzoic acid (10 mmol for each) was prepared in dry methylene chloride (25 mL). To this mixture, N, N′-dicyclohexylcarbodiimide (DCC, 10 mmol) and a small amount of 4-dimethylaminopyridine (DMAP) catalyst were added. The reaction mixture was then stirred continuously at room temperature for 72 h. Afterward, the solid that formed was filtered out, and the solution was evaporated. The resulting solid residue was purified by recrystallization from ethanol, resulting in the production of products with high purity as confirmed by thin-layer chromatography (TLC). TLC sheets coated with silica gel (E Merck) and CH_2Cl_2/CH_3OH (9:1) as the eluent were used, and only one spot was detected under a UV lamp. The structures assigned to the compounds were confirmed by 1H-NMR and elemental analyses, which showed consistent results. The ^{1}H-NMR data revealed the expected ratios of integrated aliphatic to aromatic protons for all investigated compounds. The physical data for the products, denoted as **Mn**, are listed below:

3.1.2.1 4-(2,5-Dioxo-2,5-dihydro-1H-pyrrol-1-yl)phenyl 4-(hexyloxy)benzoate M6

Yield: 91.0%; mp 108°C, ^{1}H-NMR (500 MHz, $CDCl_3$): *δ*/ppm: 0.87–0.91 (t, 3H, CH_3), 1.29–1.43 (m, 6H, $CH_3(CH_2)_3CH_2CH_2O$-), 1.72–1.74 (m, 2H, $CH_3(CH_2)_3CH_2CH_2O$-), 3.89–3.95 (t, 2H, $CH_3(CH_2)_3CH_2CH_2O$-), 7.11–7.03 (d, 2H, Ar–H), 7.30–7.38 (m, 4H, Ar–H), 7.79 (s, 2H, Pyrrole-H), 8.10–8.16 (d, 2H, Ar–H). ^{13}C-NMR (125 MHz, $CDCl_3$): *δ*/ppm: 14.1 (CH_3), 26.0, 29.3, 29.6, 31.9, 68.3 (CH_2), 121.5, 121.8, 122.4, 132.3, 132.4, 134.9, 143.0, 149.2, 159.6 (Ar-C and C=N), 163.5, 165.0 (C=O); IR (KBr): $\nu_{cm\text{-}1}$ 3041 (=C-H), 2928 (-C-H),1686, 1729 (2 C=O), 1605 (C=N), 1571 (C=C); MS, *m/z* (%) 393 (M^+, 12), 307 (100), 292 (71), 231 (63), 189 (38), 162 (81), 86 (49), 76 (71). Anal. Calcd. for $C_{23}H_{23}NO_5$ (393.44): C, 70.21; H, 5.89; N, 3.56. Found: C, 70.04; H, 5.73; N, 3.39%.

3.1.2.2 4-(2,5-Dioxo-2,5-dihydro-1*H*-pyrrol-1-yl)phenyl 4-(octyloxy)benzoate M8

Yield: 89.0%; mp 117°C, ^{1}H-NMR (500 MHz, $CDCl_3$): *δ*/ppm: 0.86–0.90 (t, 3H, CH_3), 1.28–1.44 (m, 10H, $CH_3(CH_2)_5CH_2CH_2O$-), 1.78–1.80 (m, 2H, $CH_3(CH_2)_5CH_2CH_2O$-), 3.88–3.91 (t, 2H, $CH_3(CH_2)_5CH_2CH_2O$-), 7.08–7.14 (d, 2H, Ar–H), 7.31–7.49 (m, 4H, Ar–H), 7.81 (s, 2H, Pyrrole-H), 8.11–8.13 (d, 2H, Ar–H); ^{13}C-NMR (125 MHz, $CDCl_3$): *δ*/ppm: 14.0 (CH_3), 22.5, 25.3, 25.7, 29.1, 29.3, 29.6, 29.7, 29.8, 29.9, 31.7, 68.4 (CH_2), 121.5, 121.9, 122.2, 123.0, 130.7, 133.8, 142.6, 148.9, 159.1 (Ar-C and C=N), 163.3, 164.8 (C=O); IR (KBr): $\nu_{cm\text{-}1}$ 3037 (=C-H), 2923 (-C-H), 1683, 1726 (2 C=O), 1601 (C=N), 1568 (C=C); MS, *m/z* (%) 421 (M^+, 25), 307 (100), 248 (52), 173 (80), 162 (38), 97 (53), 76 (66). Anal. Calcd. for $C_{25}H_{27}NO_5$ (421.49): C, 71.24; H, 6.46; N, 3.32. Found: C, 71.04; H, 6.28; N, 3.23%.

3.1.2.3 4-(2,5-Dioxo-2,5-dihydro-1*H*-pyrrol-1-yl)phenyl 4-(decyloxy)benzoate M10

Yield: 92.0%; mp 113°C, ^{1}H-NMR (500 MHz, $CDCl_3$): *δ*/ppm: 0.79–0.81 (t, 3H, CH_3), 1.21–1.41 (m, 14H, $CH_3(CH_2)_7CH_2CH_2O$-), 1.71–1.75 (m, 2H, $CH_3(CH_2)_7CH_2CH_2O$-), 3.81–3.96 (t, 2H, $CH_3(CH_2)_7CH_2CH_2O$-), 7.13–7.20 (d, 2H, Ar–H), 7.29–7.42 (m, 4H, Ar–H), 7.79 (s, 2H, Pyrrole-H), 8.10–8.13 (d, 2H, Ar–H). ^{13}C-NMR (125 MHz, $CDCl_3$): *δ*/ppm: 14.1 (CH_3), 22.7, 25.9, 29.1, 29.3, 29.5, 29.6, 29.7, 31.9, 68.3 (CH_2), 121.1, 121.4, 121.8, 122.4, 132.3, 134.9, 143.0, 149.2, 159.6 (Ar-C and C=N), 163.5, 164.2 (C=O); IR (KBr): $\nu_{cm\text{-}1}$ 3039 (=C-H), 2920 (-C-H), 1680, 1722 (2 C=O), 1603 (C=N), 1568 (C=C); MS, *m/z* (%) 449 (M^+, 21), 307 (100), 276 (47), 173 (63), 142 (55), 76 (61). Anal. Calcd. for $C_{27}H_{31}NO_5$ (449.55): C, 72.14; H, 6.95; N, 3.12. Found: C, 72.03; H, 6.79; N, 3.00%.

3.1.2.4 4-(2,5-Dioxo-2,5-dihydro-1*H*-pyrrol-1-yl)phenyl 4-(dodecyloxy)benzoate M12

Yield: 90%; mp 93°C, ^{1}H-NMR (500 MHz, $CDCl_3$): *δ*/ppm: 0.73–0.75 (t, 3H, CH_3), 1.10–1.35 (m, 18H, $CH_3(CH_2)_9CH_2CH_2O$-), 1.59–1.69 (m, 2H, $CH_3(CH_2)_9CH_2CH_2O$-), 3.85–3.92 (t, 2H, $CH_3(CH_2)_9CH_2CH_2O$-), 7.10–7.13 (d, 2H, Ar–H), 7.40–7.48 (m, 4H, Ar–H), 7.81 (s, 2H, Pyrrole-H), 8.13–8.17 (d, 2H, Ar–H); ^{13}C-NMR (125 MHz, $CDCl_3$): *δ*/ppm: 14.1 (CH_3), 22.7, 25.6, 25.9, 29.3, 29.5, 29.6, 29.7, 29.7, 29.8, 31.9, 68.3 (CH_2), 121.1, 121.4, 122.4, 123.2, 132.2, 134.9, 143.0, 149.4, 159.6 (Ar-C and C=N), 163.5, 165.0 (C=O); IR (KBr): $\nu_{cm\text{-}1}$ 3025 (=C-H), 2917 (-C-H), 1681, 1719 (2 C=O), 1600 (C=N), 1545 (C=C); MS, *m/z* (%) 477 (M^+, 18), 307 (100), 247 (52), 173 (46), 97 (83), 76 (51). Anal. Calcd. for $C_{29}H_{35}NO_5$ (477.60): C, 72.93; H, 7.39; N, 2.93. Found: C, 72.82; H, 7.31; N, 2.85%.

4 Conclusion

In this study, 4-(2,5-dioxo-2,5-dihydro-1*H*-pyrrol-1-yl)phenyl 4-(alkoxy)benzoates (**Mn**), a novel optical liquid crystalline homologue based on the maleic anhydride molecule, was created and mesomorphically examined using DSC and POM. Mesomorphic and optical characterizations showed that all of the studied set's produced compounds are monomorphic and display enantiotropic liquid crystalline N mesophases. A wide range of N stability has also been provided by the addition of a heterocyclic moiety to the molecular structure. The entropy increases associated with the N-isotropic transitions are minor in magnitude and follow an erratic trend that is independent of the terminal alkoxy chain length (n). This may be due to the comparatively high clearing temperature values and the smallest promotion of molecular biaxiality by the ester linkage group. Finally, it was established that the substitution under investigation causes the formation of nematic phases by contrasting the materials under investigation with their related furan compounds described in the literature.

Data availability statement

The original contributions presented in the study are included in the article/Supplementary Material, further inquiries can be directed to the corresponding author.

Author contributions

HA: Formal Analysis, Investigation, Methodology, Supervision, Validation, Writing–original draft, Writing–review and editing. SG: Methodology, Resources, Writing–original draft, Writing–review and editing. TA: Data curation, Formal Analysis, Validation, Writing–original draft. YI: Funding acquisition, Investigation, Project administration, Resources, Writing–original draft. AA: Formal Analysis, Investigation, Validation, Writing–original draft. KA: Data curation, Investigation, Writing–original draft, Writing–review and editing. MI: Conceptualization, Formal Analysis, Resources, Writing–original draft.

Funding

The author(s) declare financial support was received for the research, authorship, and/or publication of this article. This work has been financially supported by Deanship of Scientific Research in Islamic University of Madinah, Saudi Arabia the Research Groups Grant (First Call): Number 945.

Conflict of interest

The authors declare that the research was conducted in the absence of any commercial or financial relationships that could be construed as a potential conflict of interest.

Publisher's note

All claims expressed in this article are solely those of the authors and do not necessarily represent those of their affiliated organizations, or those of the publisher, the editors and the reviewers. Any product that may be evaluated in this article, or claim that may be made by its manufacturer, is not guaranteed or endorsed by the publisher.

Supplementary material

The Supplementary Material for this article can be found online at: https://www.frontiersin.org/articles/10.3389/fchem.2023.1287883/full#supplementary-material

References

Abdou, M. M., Younis, O., and El-Katori, E. E. (2022). Synthesis, experimental and theoretical studies of two aryl-azo derivatives clubbed with 2-acetylphenol and their application as novel luminescent coatings with high anticorrosion efficiency. *J. Mol. Liq.* 360, 119506. þ. doi:10.1016/j.molliq.2022.119506

Acero, N., Braña, M. F., Añorbe, L., Domínguez, G., Muñoz-Mingarro, D., Mitjans, F., et al. (2012). Synthesis and biological evaluation of novel indolocarbazoles with anti-angiogenic activity. *Eur. J. Med. Chem.* 48, 108–113. doi:10.1016/j.ejmech.2011.11.040

Ahmed, A., Abdalla, E., and Shaban, M. (2020). Simple and low-cost synthesis of Ba-doped CuO thin films for highly efficient solar generation of hydrogen. *J. Phys. Chem.* 124, 22347–22356. doi:10.1021/acs.jpcc.0c04760

Ahmed, S., and Fatima, S. (2014). Synthesis of some new maleimide derivatives. *J. Applicable Chem.* 3, 56–63.

Alaa, A. M. (2007a). Novel and versatile methodology for synthesis of cyclic imides and evaluation of their cytotoxic, DNA binding, apoptotic inducing activities and molecular modeling study. *Eur. Med. Chem.* 42, 614–626. doi:10.1016/j.ejmech.2006.12.003

Alaa, A. M. (2007b). Novel and versatile methodology for synthesis of cyclic imides and evaluation of their cytotoxic, DNA binding, apoptotic inducing activities and molecular modeling study. *Eur. J. Med. Chem.* 42, 614–626. doi:10.1016/j.ejmech.2006.12.003

Alamro, F. S., Ahmed, H. A., Bedowr, N. S., Khushaim, M. S., and El-Atawy, M. A. (2022). New advanced liquid crystalline materials bearing bis-azomethine as central spacer. *Polymers* 14, 1256. þ. doi:10.3390/polym14061256

Alamro, F. S., Gomha, S. M., Shaban, M., Altowyan, A. S., Abolibda, T. Z., and Ahmed, H. A. (2021). Optical investigations and photoactive solar energy applications of new synthesized Schiff base liquid crystal derivatives. *Sci. Rep.* 11, 15046. þ. doi:10.1038/s41598-021-94533-6

Alshabanah, L. A., Al-Mutabagani, L. A., Gomha, S. M., Ahmed, H. A., Popoola, S. A., and Shaban, M. (2021). Novel sulphonic acid liquid crystal derivatives: experimental, computational and optoelectrical characterizations. *RSC Adv.* 11, 27937–27949. þ. doi:10.1039/d1ra02517a

Attard, G., Date, R., Imrie, C. T., Luckhurst, G. R., Roskilly, S. J., Seddon, J. M., et al. (1994). Non-symmetric dimeric liquid crystals the preparation and properties of the α-(4-cyanobiphenyl-4′-yloxy)-ω-(4-*n*-alkylanilinebenzylidene-4′-oxy)alkanes. *Liq. Cryst.* 16, 529–581. doi:10.1080/02678299408036531

Badru, R., Anand, P., and Singh, B. (2012). Synthesis and evaluation of hexahydropyrrolo [3, 4-d] isoxazole-4, 6-diones as anti-stress agents. *Eur. J. Med. Chem.* 48, 81–91. doi:10.1016/j.ejmech.2011.11.037

Behera, P. K., Rao, S., Popoola, L. T., Swamirayachar, S. A., AlFalah, M. G. K., Kandemirli, F., et al. (2023). Room temperature columnar liquid crystalline perylene bisimide as a novel corrosion resistant surface film for mild steel surface. *J. Bio-and Tribo-Corrosion* 9, 18. þ. doi:10.1007/s40735-022-00735-4

Benicewicz, B. C., Smith, M. E., Langlois, D. A., Gavrin, A. J., and Douglas, E. P. (1997). Bisacetylene liquid crystalline thermosets with flexible tails. *Polym. Prepr. America* 38, 307–308.

Bharel, R., Choudhary, V., and Varma, I. K. (1993). Thermal and mechanical properties of copolymers of methyl methacrylate with N-phenyl maleimide. *J. Appl. Polym. Sci.* 49, 31–38. doi:10.1002/app.1993.070490105

Birkinshaw, J. H., Kalyanpur, M. G., and Stickings, C. E. (1963). Studies in the biochemistry of micro-organisms. 113. Pencolide, a nitrogen-containing metabolite of Penicillium multicolor Grigorieva-Manilova and Poradielova. *Biochem. J.* 86, 237–243. doi:10.1042/bj0860237

Bojarski, A. J., Mokrosz, M. J., Duszyńska, B., Kozioł, A., and Bugno, R. (2004). New imide 5-HT1A receptor ligands–modification of terminal fragment geometry. *Molecules* 9, 170–177. doi:10.3390/90300170

Burtoloso, A. C. B., Garcia, A. L., Miranda, K. C., and Correia, C. R. D. (2006). Heck arylation of maleic anhydrides using arenediazonium tetrafluoroborates: synthesis of mono-and diarylated maleic anhydrides and of the marine alkaloids prepolycitrin A and polycitrin A. *Synlett* 2006, 3145–3149. doi:10.1055/s-2006-951524

Carfagna, C., Amendola, E., and Giamberini, M. (1994a). Rigid rod networks: liquid crystalline epoxy resins. *Compos. Struct.* 27 (1-2), 37–43. doi:10.1016/0263-8223(94)90064-7

Carfagna, C., Amendola, E., and Giamberini, M. (1994b). Liquid crystalline epoxy resins containing binaphthyl group as rigid block with enhanced thermal stability. *Macromol. Chem. Phys.* 195, 2307–2315. doi:10.1002/macp.1994.021950703

Carfagna, C., Amendola, E., Giamberini, M., Hakemi, H., and Pane, S. (1997). Liquid crystalline epoxy resins in polymer dispersed liquid crystal composites. *Polym. Iternational* 44, 465–473. doi:10.1002/(sici)1097-0126(199712)44:4<465::aid-pi850>3.0.co;2-x

Chen, H. J., Liu, Y., Wang, L. N., Shen, Q., Li, J., and Nan, F. J. (2010). Discovery and structural optimization of pyrazole derivatives as novel inhibitors of Cdc25B. *Bioorg. Med. Chem. Lett.* 20, 2876–2879. doi:10.1016/j.bmcl.2010.03.040

Chigrinov, V. G., Belyaev, V. V., Kozenkov, V. M., Chausov, D. N., Margaryan, H. L., Hakobyan, N. H., et al. (2022). Azodyes for liquid crystal photoalignment in displays and diffraction optical elements. *Emerg. Liq. Cryst. Technol. XVII* 12023, 26–36. doi:10.1117/12.2614534

Cho, S. H., Lee, J. Y., and Douglas, E. P. (2006). Synthesis and thermal properties of liquid crystalline thermoset containing rigid-rod epoxy. *High. Perform. Polym.* 18, 83–99. doi:10.1177/0954008306056484

Domszy, R. C., and Shannon, P. J. (1990). Thermotropic polyesters based on trans-1, 4-cyclohexane dicarboxylate mesogens and flexible spacer groups. *Macromolecules* 23, 2790–2797. doi:10.1021/ma00212a033

Dürüst, Y., Karakuş, H., Kaiser, M., and Tasdemir, D. (2012). Synthesis and anti-protozoal activity of novel dihydropyrrolo [3, 4-d] [1, 2, 3] triazoles. *Eur. J. Med. Chem.* 48, 296–304. doi:10.1016/j.ejmech.2011.12.028

Gavrin, A. J., and Douglas, E. P. (2001). Isothermal curing of acetylene functionalized liquid crystalline thermoset monomers. *Macromolecules* 34, 5876–5884. doi:10.1021/ma001884+

Ghosh, T., and Lehmann, M. (2017). Recent advances in heterocycle-based metal-free calamitics. *J. Mater. Chem. C* 5 (47), 12308–12337. doi:10.1039/c7tc03502k

Gomha, S. M., Ahmed, H. A., Shaban, M., Abolibda, T. Z., Alharbi, K. A., and Alalawy, H. H. (2021). New nematogenic conical-shaped supramolecular H-bonded complexes for solar energy investigations. *Sci. Rep.* 11, 17622. þ. doi:10.1038/s41598-021-97126-5

Gordon, A. J., and Ehrenkaufer, R. L. E. (1971). Chemistry of imides. II. Cyclic imides and some unusual products from some diacid chlorides and lithium nitride. *J. Org. Chem.* 36 (1), 44–45. doi:10.1021/jo00800a011

Gray, G. W. (1962). *Molecular structure and the properties of liquid crystals*. Cambridge, Massachusetts, United States: Academic Press.

Ha, S. T., Koh, T. M., Lee, S. L., Yeap, G. Y., Lin, H. C., and Ong, S. T. (2010). Synthesis of new schiff base ester liquid crystals with a benzothiazole core. *Liq. Cryst.* 37, 547–554. doi:10.1080/02678291003710425

Hamper, B. C., Dukesherer, D. R., and South, M. S. (1996). Solid-phase synthesis of proline analogs via a three component 1, 3-dipolar cycloaddition. *Tetrahedron Lett.* 37, 3671–3674. doi:10.1016/0040-4039(96)00659-4

Han, J. (2013). 1, 3, 4-Oxadiazole based liquid crystals. *J. Mater. Chem. C* 1 (47), 7779–7797. doi:10.1039/c3tc31458h

Handley, G. J., Nelson, E. R., and Somers, T. C. (1960). Compounds derived from β-substituted glutaric acids: glutarimides, glutaramic acids, 1, 5-pentane diols. *Aust. J. Chem.* 13, 129–144. doi:10.1071/ch9600129

Hasegawa, M., Tanaka, Y., Koseki, K., and Tominaga, A. (2006). Positive-type photo-patterning of low-CTE, high-modulus transparent polyimide systems. *J.Photopolymer Sci. Technol.* 19, 285–290. doi:10.2494/photopolymer.19.285

Hasegawa, M., and Tominaga, A. (2005). Environmentally friendly positive-and negative-tone photo-patterning systems of low-K and low-CTE polyimides. *J. Photopolym. Sci. Technol.* 18, 307–312. doi:10.2494/photopolymer.18.307

Henderson, P. A., Seddon, J. M., and Imrie, C. T. (2005). Methylene-and ether-linked liquid crystal dimers II. Effects of mesogenic linking unit and terminal chain length. *Liq. Cryst.* 32, 1499–1513. doi:10.1080/02678290500284983

Hoyt, A. E., Benicewicz, B. C., and Huang, S. J. (1990a). *Liquid-crystalline polymers*. Washington, DC, USA: Am. Chem. Soc., Rigid rod molecules as liquid crystal thermosets.

Hoyt, A. E., Benicewicz, B. C., and Huang, S. J. (1990b). *Liquid-crystalline polymers*. Washington, DC, USA: Am. Chem. Soc., Rigid rod molecules as liquid crystal thermosets.

Iijima, T., Suzuki, N., Fukuda, W., and Tomoi, M. (1995). Toughening of aromatic diamine-cured epoxy resins by modification with N-phenylmaleimide-styrene-p-hydroxystyrene terpolymers. *Eur.Polymer J.* 31, 775–783. doi:10.1016/0014-3057(95)00019-4

Jang, J., and Bae, J. (2005). Formation of polyaniline nanorod/liquid crystalline epoxy composite nanowires using a temperature-gradient method. *Adv. Funct. Mater.* 15, 1877–1882. doi:10.1002/adfm.200400608

Jcashman, J. R., MacDonald, M., Ghirmai, S., Okolotowicz, K. J., Sergienko, E., Brown, B., et al. (2010). Inhibition of bfl-1 with N-aryl maleimides. *Bioorg. Med. Chem. Lett.* 20, 6560–6564. doi:10.1016/j.bmcl.2010.09.046

Langlois, D. A., Benicewicz, B. C., and Douglas, E. P. (1994). Synthesis, phase behavior, and curing studies of bisacetylene rigid-rod thermosets. *Chem. Mater.* 6, 1925–1933. doi:10.1021/cm00047a007

Langmuir, M. E., Yang, J. R., Moussa, A. M., Laura, R., and LeCompte, K. A. (1995). New naphthopyranone based fluorescent thiol probes. *Tetrahedron Lett.* 36, 3989–3992. doi:10.1016/0040-4039(95)00695-9

Lee, J. Y. (2006). Relationship between anisotropic orientation and curing of liquid crystalline epoxy resin. *J. Appl. Polym. Sci.* 102, 1712–1716. doi:10.1002/app.24352

Lee, J. Y., Shim, M. J., and Kim, S. W. (2002). Synthesis of liquid crystalline epoxy and its mechanical and electrical characteristics—curing reaction of LCE with diamines by DSC analysis. *J. Appl. Polym. Sci* 83, 2419–2425. doi:10.1002/app.10204

Li, H., Wu, Q., Zhou, R., Shi, Y., Yang, C., Zhang, Y., et al. (2019). Liquid-crystalline small molecules for nonfullerene solar cells with high fill factors and power conversion efficiencies. *Adv. Energy Mater.* 9, 1803175. þ. doi:10.1002/aenm.201803175

López, S. N., Sortino, M., Escalante, A., de Campos, F., Corrêa, R., Cechinel Filho, V., et al. (2003). Antifungal properties of novel N- and α,β-substituted succinimides against dermatophytes. *Arzneimittelforschung* 53 (04), 280–288. doi:10.1055/s-0031-1297109

Luckhurst, G., and Gray, G. W. (1979). *The molecular physics of liquid crystals*. Cambridge, Massachusetts, United States: Academic Press.

Ma, J., Choi, J., Park, S., Kong, I., Kim, D., Lee, C., et al. (2023). Liquid crystals for advanced smart devices with microwave and millimeter-wave applications: recent progress for next-generation communications. *Adv. Mater.*, 2302474. þ. doi:10.1002/adma.202302474

Mahle, F., Guimaraes, T., Meira, A., Correa, R., Cruz, R., Nunes, R., et al. (2010). Synthesis and biological evaluation of N-antipyrine-4-substituted amino-3-chloromaleimide derivatives. *Eur. J. Med. Chem.* 45, 4761–4768. doi:10.1016/j.ejmech.2010.07.040

Mallon, J. J., and Adams, P. M. (1993). Synthesis and characterization of novel epoxy monomers and liquid crystal thermosets. *J. Polym. Sci. Part A Polym. Chem.* 31, 2249–2260. doi:10.1002/pola.1993.080310908

Matuszak, N., Muccioli, G. G., Labar, G., and Lambert, D. M. (2009). Synthesis and *in vitro* evaluation of N-substituted maleimide derivatives as selective monoglyceride lipase inhibitors. *J. Med. Chem.* 52, 7410–7420. doi:10.1021/jm900461w

Merlo, A. A., Tavares, A., Khan, S., Leite Santos, M. J., and Teixeira, S. R. (2018). Liquid-crystalline coumarin derivatives: contribution to the tailoring of metal-free sensitizers for solar cells. *Liq. Cryst.* 45, 310–322. doi:10.1080/02678292.2017.1324644

Mohammed, I. A., and Mustapha, A. (2010a). Synthesis of new azo compounds based on N-(4-hydroxypheneyl) maleimide and N-(4-methylpheneyl) maleimide. *Molecules* 15, 7498–7508. doi:10.3390/molecules15107498

Mohammed, I. A., and Mustapha, A. (2010b). Synthesis of new azo compounds based on N-(4-Hydroxypheneyl)maleimide and N-(4-Methylpheneyl)maleimide. *Molecules* 15, 7498–7508. doi:10.3390/molecules15107498

Morita, Y., Arakawa, K., Todo, M., and Kaneto, M. (2006). Experimental study on the thermo-mechanical effects of underfill and low-CTE substrate in a flip-chip device. *Microelectron. Reliab.* 46, 923–929. doi:10.1016/j.microrel.2005.02.013

Mormann, W., and Zimmermann, J. (1995). Synthesis and mesogenic properties of diaromatic cyanates and isocyanates-monomers for liquid crystalline thermosets. *Liq. Cryst.* 19, 227–233. doi:10.1080/02678299508031973

Nafee, S. S., Ahmed, H. A., and Hagar, M. (2020a). Theoretical, experimental and optical study of new thiophene-based liquid crystals and their positional isomers. *Liq. Cryst.* 47, 1291–1302. doi:10.1080/02678292.2019.1710778

Nafee, S. S., Ahmed, H. A., and Hagar, M. (2020b). Theoretical, experimental and optical study of new thiophene-based liquid crystals and their positional isomers. *Liq. Cryst.* 47, 1291–1302. doi:10.1080/02678292.2019.1710778

Nayak, R. A., Bhat, S. A., Shanker, G., Rao, D. S., and Yelamaggad, C. V. (2019). Highly frustrated liquid crystal phases in optically active dimers: synthesis and rich phase transitional behavior. *New J. Chem.* 43 (5), 2148–2162. þ. doi:10.1039/c8nj03520b

Ohkubo, M., Nishimura, T., Jona, H., Honma, T., and Morishima, H. (1996). Practical synthesis of indolopyrrolocarbazoles. *Tetrahedron* 52 (24), 8099–8112. doi:10.1016/0040-4020(96)00372-9

Połoński, T., Milewska, M. J., and Gdaniec, M. (2000). Synthesis, structure and chiroptical spectra of the bicyclic α-diketones, imides and dithioimides related to santenone. *Tetrahedron Asymmetry* 11, 3113–3122. doi:10.1016/s0957-4166(00)00283-4

Pradhan, B., Chakraborty, N., Gupta, R. K., Shanker, G., and Achalkumar, A. S. (2017). Nonsymmetrical cholesterol dimers constituting regioisomeric oxadiazole and thiadiazole cores: an investigation of the structure–property correlation. *New J. Chem.* 41 (2), 879–888. þ. doi:10.1039/c6nj03141b

Ren, L., Duan, L., Weng, Q., Chen, P., Gao, A., Chen, X., et al. (2019). Synthesis and study the liquid crystalline properties of compounds containing benzoxazole core and terminal vinyl group. *Liq. Cryst.* 46, 797–805. doi:10.1080/02678292.2018.1530383

Seed, A. (2007). Synthesis of self-organizing mesogenic materials containing a sulfur-based five-membered heterocyclic core. *Chem. Soc. Rev.* 36 (12), 2046–2069. doi:10.1039/b612666a

Shanker, G., and Yelamaggad, C. V. (2011). A new class of low molar mass chiral metallomesogens: synthesis and characterization. *J. Mater. Chem.* 21 (39), 15279–15287. þ. doi:10.1039/c1jm11947h

Sivaprakasam, P., Xie, A., and Doerksen, R. J. (2006). Probing the physicochemical and structural requirements for glycogen synthase kinase-3α inhibition: 2D-QSAR for 3-anilino-4-phenylmaleimides. *Bioorg. Med. Chem.* 14, 8210–8218. doi:10.1016/j.bmc.2006.09.021

Sorai, M., and Saito, K. (2003). Alkyl chains acting as entropy reservoir in liquid crystalline materials. *Chem. Rec.* 3, 29–39. doi:10.1002/tcr.10046

Stewart, S. G., Polomska, M. E., and Lim, R. W. (2007). A concise synthesis of maleic anhydride and maleimide natural products found in Antrodia camphorata. *Tetrahedron let.* 48 (13), 2241–2244. doi:10.1016/j.tetlet.2007.01.169

Sunil, B. N., Srinatha, M. K., Shanker, G., Hegde, G., Alaasar, M., and Tschierske, C. (2020). Effective tuning of optical storage devices using photosensitive bent-core liquid crystals. *J. Mol. Liq.* 304, 112719. þ. doi:10.1016/j.molliq.2020.112719

Suzuki, T., Tanaka, R., Hamada, S., Nakagawa, H., and Miyata, N. (2010). Design, synthesis, inhibitory activity, and binding mode study of novel DNA methyltransferase 1 inhibitors. *Bioorg. Med. Chem. Lett.* 20, 1124–1127. doi:10.1016/j.bmcl.2009.12.016

Tariq, M., Hameed, S., Bechtold, I. H., Bortoluzzi, A. J., and Merlo, A. A. (2013). Synthesis and characterization of some novel tetrazole liquid crystals. *J.Materials Chem. C* 1 (35), 5583–5593. doi:10.1039/c3tc30966e

Uchida, J., Soberats, B., Gupta, M., and Kato, T. (2022). Advanced functional liquid crystals. *Adv. Mater.* 34, 2109063. þ. doi:10.1002/adma.202109063

Wang, H., Zhou, H., He, W., Yang, Z., Cao, H., Wang, D., et al. (2022). Research progress on blue-phase liquid crystals for pattern replication applications. *Materials* 16, 194. þ. doi:10.3390/ma16010194

Wang, Z. D., and Jiang, S. Q. (2006). Coefficient of thermal expansion of stressed thin films. *Trans. Nonferrous Metals Soc. China* 16, s220–s225. doi:10.1016/s1003-6326(06)60179-9

Weng, Q., Duan, L., Chen, P., Gao, A., Chen, X., and An, Z. (2019b). Synthesis and mesomorphic properties of the nematic mesophase benzoxazole derivatives with big twist angle of difluoro-biphenyl unit. *Liq. Cryst.* 46 (7), 1013–1023. doi:10.1080/02678292.2018.1550818

Weng, Q., Duan, L., Chen, P., Shi, D., Gao, A., Chen, X., et al. (2019a). Synthesis and mesomorphic properties of benzoxazole derivatives with lateral multifluoro substituents. *Liq. Cryst.* 46 (1), 59–66. doi:10.1080/02678292.2018.1468501

Wu, C. S., Liu, Y. L., and Hsu, K. Y. (2003). Maleimide-epoxy resins: preparation, thermal properties, and flame retardance. *Polymer* 44, 565–573. doi:10.1016/s0032-3861(02)00812-1

Yeap, C. W., Haque, R. A., Yam, W. S., and Razali, M. R. (2018). Asymmetric N-heterocyclic carbene benzimidazolium salts and their silver (I) complexes: potential as ionic liquid crystals. *Liq. Cryst.* 45, 1210–1222. doi:10.1080/02678292.2018.1426127

Yeap, G. Y., Lee, H. C., Mahmood, W. A. K., Imrie, C. T., Takeuchi, D., and Osakada, K. (2011). Synthesis, thermal and optical behaviour of non-symmetric liquid crystal dimers α-(4-benzylidene-substituted-aniline-4′-oxy)-ω-[pentyl-4-(4′-phenyl) benzoateoxy]hexane. *Phase Transitions* 84, 29–37. doi:10.1080/01411594.2010.513613

Yeap, G. Y., Osman, F., and Imrie, C. T. (2015). Non-symmetric dimers: effects of varying the mesogenic linking unit and terminal substituent. *Liq. Cryst.* 42, 543–554. doi:10.1080/02678292.2015.1004843

Yelamaggad, C. V., and Shanker, G. (2007). Synthesis and characterization of non-symmetric chiral dimers. *Liq. Crystfals* 34 (9), 1045–1057. þ. doi:10.1080/02678290701616280

Yin, K., Hsiang, E. L., Zou, J., Li, Y., Yang, Z., Yang, Q., et al. (2022). Advanced liquid crystal devices for augmented reality and virtual reality displays: principles and applications. *Light Sci. Appl.* 11, 161. þ. doi:10.1038/s41377-022-00851-3

Zhang, G., Zhao, J., Chow, P. C., Jiang, K., Zhang, J., Zhu, Z., et al. (2018). Nonfullerene acceptor molecules for bulk heterojunction organic solar cells. *Chem. Rev.* 118, 3447–3507. þ. doi:10.1021/acs.chemrev.7b00535